

Spatial variability of residual nitrate-nitrogen under two tillage systems in central Iowa: A composite three-dimensional resistant and exploratory approach

B. P. Mohanty¹ and R. S. Kanwar

Department of Agricultural and Biosystems Engineering, Iowa State University, Ames

Abstract. Soil nitrate-nitrogen ($\text{NO}_3\text{-N}$) data arranged on a three-dimensional grid were analyzed to compare tillage effect on the spatial distribution of residual $\text{NO}_3\text{-N}$ in the soil profile of agricultural plots drained by subsurface tiles. A three-dimensional median-based resistant (to outlier(s)) approach was developed to polish the spatially located data on soil $\text{NO}_3\text{-N}$ affected by directional trends (nonstationarity in the mean) in three major directions (row, column, and depth) and along the horizontal diagonal directions of the grid. Effect of preferential or nonpreferential path of transport of $\text{NO}_3\text{-N}$ in the vertical direction defined as sample hole effect was also removed to make the data trend-free across holes. Composite three-dimensional semivariogram models (along horizontal and vertical directions) were used to describe the spatial structure of residual soil nitrate distribution. Two plots in the same field, one under each tillage system (conventional tillage and no tillage), were studied. In each plot, soil samples were collected at five depths (30, 60, 90, 120, and 150 cm) from 35 sites (holes) arranged on a 7×5 regular grid of 7.6×7.6 m. In the conventional tillage plot, residual $\text{NO}_3\text{-N}$ concentrations decreased gradually to a depth of 90 cm and increased beyond this depth. The coefficient of variation, however, became gradually smaller, showing more uniform distribution for greater depths. In the no-tillage plot, trends were similar to those in the conventional tillage system, but were spatially more stable across the profile. Structural analyses indicated that under conventional tillage, the semivariogram of residual soil nitrate distribution was linear in the horizontal and vertical directions. In contrast, the semivariograms for no-tillage showed nugget-type behavior, indicating a lack of spatial structure in the residual soil nitrate.

Introduction

In recent years, increased public concern about water quality has heightened interest in the efficient use of nitrogen for agricultural production systems. Studies have indicated that nitrogen application rates in agricultural fields are often much higher than the crops can use. Therefore the unused nitrogen either leaves the system through leaching, washoff, and volatilization or remains in the soil profile for possible leaching to groundwater. Knowledge of spatial structures and other inducing factors for residual nitrate distribution in the soil profile under different tillage practices is useful to understand its transport, transformation, and retention pattern. This will help researchers developing new tillage-based nitrogen management practices to enhance groundwater quality.

Transport, transformation, and distribution of nitrate-nitrogen ($\text{NO}_3\text{-N}$) under different field conditions depend upon physical, biological, and chemical processes occurring in the soil profile. Other factors responsible for the spatial distribution of $\text{NO}_3\text{-N}$ are water and solute displacement under nonsteady flow conditions along preferential and

nonpreferential flow paths, variable water table depth causing nitrification and denitrification, nitrogen transformations by enzymatic and bacterial pathways, plant uptake of water and nitrogen, and soil texture [Wagenet and Rao, 1983]. Studies conducted by Burrough [1983], Wagenet and Rao [1983], and Tabor *et al.* [1985] indicate that each of these factors may operate either independently or in conjunction with others to cause abrupt or gradual changes in nitrogen transport and retention. These factors must be considered when studying the spatial behavior of residual $\text{NO}_3\text{-N}$ in the soil profile. Several studies [Walker and Brown, 1983; Rao *et al.*, 1983, 1985; Rao and Wagenet, 1985] have examined the spatial variability and its intrinsic factors influencing herbicide degradation rates in the soil profile. Villeneuve *et al.* [1988] pointed out the intrinsic and extrinsic variability of soil chemical properties. For instance, the spatial variability of soil organic matter is closely linked to the variability of soil composition and structure, which derives from soil pedogenesis. Spatial variability of a pesticide concentration or flux in soil, which is due to cultivation and pesticide application practices, leads to a variation in the adsorption and degradation parameters.

Macropores are responsible for solute movement [Beven and Germann, 1982]. Trojan and Linden [1992] report that macropore distribution (spatially and along depth), length (vertically), continuity (vertically), and tortuosity (vertically) are functions of depth and affect the spatial variability of residual/sorbed solutes (e.g., pesticides). Singh *et al.* [1991]

¹Now at U.S. Salinity Laboratory, Agricultural Research Service, U.S. Department of Agriculture, Riverside, California.

showed the tillage-induced differences in spatial and vertical distribution, length, and continuity of macropores under conventional and no-tillage practices. Many researchers [Gast *et al.*, 1978; Baker *et al.*, 1975; Baker *et al.*, 1989; Kanwar *et al.*, 1985, 1988; Kanwar and Baker, 1991; Kanwar, 1991] have studied the accumulation of $\text{NO}_3\text{-N}$ in soil profiles and $\text{NO}_3\text{-N}$ loss with tile drainage water under continuous corn as a function of different tillage practices, but spatial structure and variability of residual $\text{NO}_3\text{-N}$ in these fields have not been studied.

The objective of this study was to compare the spatial distribution of residual $\text{NO}_3\text{-N}$ in the (tile) drained soil profile under conventional tillage and no-tillage systems, by using a three-dimensional median-based resistant (little affected by data outlier(s)) approach coupled with geostatistics for the data collected on a three-dimensional spatial grid. The paper also demonstrates how three-dimensional gridded data give a clearer picture of spatial structure (composite three-dimensional semivariograms) of residual $\text{NO}_3\text{-N}$ distribution in the soil profile under different tillage practices than do two-dimensional gridded data producing two-dimensional semivariograms. Moreover, it shows how three-dimensional median polish of gridded spatial data provides a relatively simple, cost-effective, resistant, and almost bias-free procedure in the presence of trend and zonal anisotropy when compared with more general polynomial modeling and generalized least squares fitting of trend.

Previous Applications

Transport and retention capacities for water and chemicals in an agricultural field are spatially and temporally variable. Spatial variability, as used here, includes areal variations at a given depth and also variations with depth at a given location in the field. Both types of variability need to be considered when assessing the fate of $\text{NO}_3\text{-N}$ under different field conditions. Exploratory data analysis, relying on resistant measures and graphical tools, and robustness concepts in geostatistics, offer a variety of ways to model such processes as realizations of space-time random functions. Dagan [1986], Ginn and Cushman [1990], Rouhani and Wackernagel [1990], Shafer and Varljen [1990], Rubin and Journal [1991], and others have successfully applied covariance-related stochastic methods in groundwater modeling. Further efforts to develop better spatial characterization methods of water and chemical transport and retention properties seem warranted, not only in the saturated zone but also for extending these methods to transport modeling in the vadose zone. However, few studies [Russo, 1984; Unlu *et al.*, 1990] of the spatial variability of unsaturated flow parameters have concentrated on quantifying heterogeneity in the horizontal plane of fields. A recent study by Russo and Bouton [1992] focused on the spatial variability of these flow parameters in the depth direction. Cressie and Horton [1987] and Onofiok [1988] studied the tillage effect on soil water infiltration and other soil properties and observed some interesting differences.

Sweeping the localized effects by exploratory approaches [Tukey, 1977; Velleman and Hoaglin, 1981] such as row and column median polish [Hamlett *et al.*, 1986; Cressie and Horton, 1987], winsorization [Gotway and Cressie, 1990], and split-window median polish [Mohanty *et al.*, 1991] coupled with classical geostatistics [Matheron, 1963] or

robust geostatistics [Cressie and Hawkins, 1980] is becoming popular in soil science. Among others, one important advantage of these approaches is that they allow visual examination of data for normality, constancy in the mean and the variance, and trend freeness. Trends are often unverified by geologists and soil scientists, who confuse inherent spatial structure with the effects of extrinsic factors and drift [Horowitz and Hillel, 1983; Hamlett *et al.*, 1986]. In the present study, data arranged on a three-dimensional grid and resistant (to outlier(s)) schemes were investigated with the "three-way main effects only" median polish approach [Cook, 1985], an extension of "two-way" median polish [Tukey, 1977; Velleman and Hoaglin, 1981; Emerson and Hoaglin, 1983]. This approach removes trend due to crop row effects and/or other effects (parallel to grid rows), drainage tile induced water table effects at deeper depths and/or other effects at shallow depths (parallel to grid columns), and surface/subsurface soil characteristics effects and/or soil water content effects (in terms of advection and dispersion) (parallel to grid depth) from the data before spatial analyses of residual $\text{NO}_3\text{-N}$ in the soil profile were made to compare distribution patterns under conventional tillage with those under no tillage.

Experimental Design

Two 0.4-ha (1 acre) plots, each under a different tillage system (conventional tillage and no tillage), were selected at the Agronomy and Agricultural Engineering Research Center near Ames, Iowa. The plots had been continuously planted to corn under the same tillage system for 5 years and had received an application of 175 kg/ha liquid nitrogen fertilizer every year. For both plots, a single application (soon after planting) of nitrogen was adopted. Soils of these plots were Nicollet loam (fine loamy, mixed, mesic aquic Hapludolls) and Clarion loam (fine loamy, mixed, mesic typic Hapludolls) in the Nicollet-Clarion-Webster Association and had a maximum slope of 2%. Each plot was drained by a single subsurface tile drain at 120 cm depth to eliminate periodic buildup of excessive wetness.

Samples were collected from both plots by using a 5×7 grid network of 35 sites, with a regular grid spacing of 7.6 m. Sampling scheme was limited to plot boundary in horizontal directions and close to subsurface tile in the vertical direction. Soil samples were taken to a depth of 150 cm at 30-cm intervals with a 3.2-cm probe. There were 175 data points in total. Figure 1 shows the location of sampling points within the plot arranged on a three-dimensional grid. Under the practical geostatistical rule for the minimum number of pairs for semivariogram estimation [Journal and Huijbregts, 1978; N. A. C. Cressie, personal communication, 1992], our number of samples is considered adequate. The labor and budget required in conducting a study on $\text{NO}_3\text{-N}$ transport and retention in soil profile were also considered in determining the number of samples. Each soil sample represents average $\text{NO}_3\text{-N}$ over 10 cm depth at a particular spatial location (x, y, z). A sample of 10-cm length, however, was considered a point sample for the two- and one-dimensional type semivariogram estimation in horizontal directions. In vertical direction, however, regularized semivariogram models [Journal and Huijbregts, 1978, p. 80] were calculated following the theoretical model fitting, to compensate for the vertical sample length (i.e., 10 cm). Because we focused on

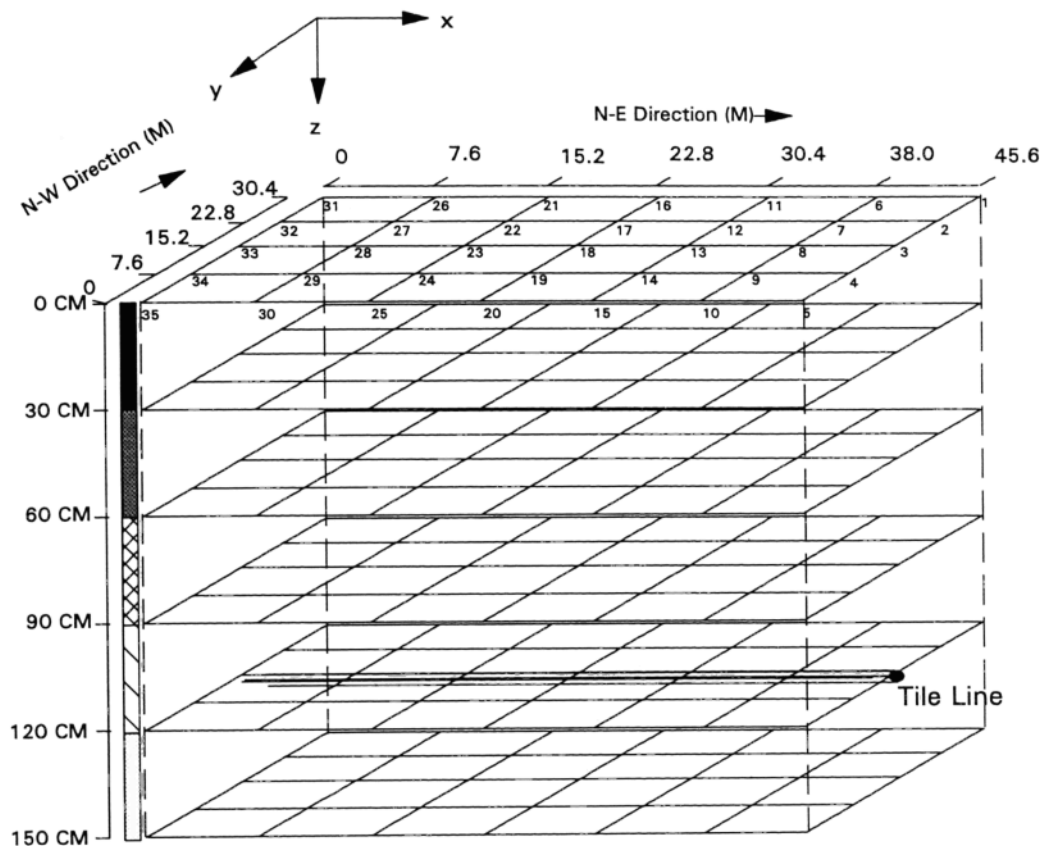


Figure 1. Arrangement of nitrate sampling locations in the experimental plots; 35 sites on a 7×5 grid and 5 depths.

the spatial behavior of residual nitrate (i.e., $\text{NO}_3\text{-N}$ retained in the soil mostly from previous crop years), samples were collected during the period when no appreciable rain fell to minimize the contribution of surface-applied nitrogen fertilizer (a few days before soil sampling). This was necessary because of the limited advection and dispersion processes occurring during this rain-free period. Thus the amount of $\text{NO}_3\text{-N}$ in the soil samples indicates mostly the residual amount retained from previous years after leaching to groundwater body and tile discharge, and uptake by plants. All samples were collected within a 13-day period in June to minimize temporal variability among samples. The samples were analyzed for soil water content and for soil water $\text{NO}_3\text{-N}$ concentration. Colorimetric automated Cadmium reduction method (EPA 353.2) was used to determine the $\text{NO}_3\text{-N}$ concentration in the soil samples.

Methodology

The objective of this study was to present simple, physically interpretable, resistant schemes for spatial analyses. The basic purpose of resistant schemes is to clean or to polish field data to satisfy the basic assumptions for the estimation of semivariograms, that is, for second-order stationarity or the weaker intrinsic hypothesis. Second-order stationarity implied that the mathematical expectation $E[Z(x)] = \mu$ exists and does not depend upon the position x and that for each pair of regionalized variables $[Z(x), Z(x + h)]$, the covariance exists and depends only upon the

separation vector h . On the other hand, the weaker intrinsic hypothesis implied that the mathematical expectation $E[Z(x)] = \mu$ exists, and for all vectors h the increment $[Z(x + h) - Z(x)]$ has a finite variance that does not depend on x [Journel and Huijbregts, 1978, p. 32]. These basic assumptions of regional variable studies, however, are often overlooked or rarely verified by researchers, who may introduce artifacts and confound the interpretation of results, as described in the work by Cressie and Horton [1987]. Therefore it is important to run a thorough data analysis before and during geostatistical analysis to filter out any site-specific potential problems (producing trends) related to the known regionalized variable (i.e., soil property under investigation).

This study was conducted to identify the physically recognizable extrinsic factors existing on the site and to isolate their effects in the distribution of residual $\text{NO}_3\text{-N}$ in the soil profile. These effects usually produce nonstationarity in the mean and the variance along the major axes of experimental design. Besides these main effects, the intrinsic/cross-product trends along the diagonal directions in a grid-type sampling pattern could also be identified and filtered out. Once spatial stationarity of the regionalized variable is attained, the measurements over all depths are combined into a composite data set, and semivariogram analyses are conducted. This study shows how easily exploratory data analysis techniques could assure crucial stationarity assumptions in regionalized variable and make the data free of extrinsic factors and intrinsic trends before further geostatistical analyses.

Exploratory Analysis

Variability in geo-related properties such as transport, transformation, and retention of $\text{NO}_3\text{-N}$ is likely to be three-dimensional in the three-dimensional space of a soil profile. In our study, we identified the effects of crop row parallel to the grid row, of tile-induced water table elevations parallel to the grid column at deeper depths, and of surface/subsurface soil and soil water content parallel to the grid depth in residual $\text{NO}_3\text{-N}$ distribution in the soil profile. Also the effects of (tillage-induced) pore size distribution, pore length, and their continuity were found in residual $\text{NO}_3\text{-N}$ distribution. Although spatial field experiments are usually designed with their grids in meaningful directions, residuals should still be checked for cross-product trends or interactions, e.g., between row and column factors, along the diagonals. Unlike a mining problem extending over great depths in which drift might occur in any direction in three-dimensional space, this study has been kept simple, and diagonal trends have been assumed only in horizontal directions because of the shallow depth (1.5 m), the limited scale (plot size, 46 m \times 31 m), and the type (vertical transport of $\text{NO}_3\text{-N}$ in the soil profile) of the problem. *Scheffe* [1959, p. 130] and *Cressie* [1991, p. 190] modeled this diagonal trend through an extra parameter g in the additive models, which accounts for a quadratic term in the fit. Consequently, this study, a modified three-dimensional additive model based on *Cook's* [1985] "three-way main effects only" model and *Cressie's* [1991] diagonal drift term was developed:

$$Z_{ijk} = \mu + \alpha_i + \beta_j + \xi_k + g(x_i - \bar{x})(y_j - \bar{y}) + \varepsilon_{ijk}, \quad (1)$$

$$i = 1, \dots, I \quad j = 1, \dots, J; \quad k = 1, \dots, K,$$

where

- Z_{ijk} regionalized variable (residual $\text{NO}_3\text{-N}$) of the cell (i, j, k) corresponding to row i , column j , and layer (depth) k ;
- μ common value;
- α_i row effect (i.e., crop row effect and/or other effect);
- β_j column effect (i.e., elliptical water table effect and/or other effect);
- ξ_k layer effect (i.e., surface/subsurface soil effect and/or soil water content effect);
- g diagonal drift parameter;
- \bar{x} ave $\{x_i, i = 1 \dots I\}$;
- \bar{y} ave $\{y_j, j = 1 \dots J\}$;
- ε_{ijk} a random component that may or may not inherit the spatial structure of the property (residual $\text{NO}_3\text{-N}$ under the tillage practice) in study in cell (i, j, k).

Median Polish

Representing the raw (for more normally distributed) or \log_e -transformed (for more lognormally distributed) data by a modified additive model will lead to an interpretation of a combined output of some stochastic random fluctuation and deterministic physical realities existing at a particular site. The next logical step would be to remove the effects of these physical factors (i, j, k , and ij) one by one to leave behind the residual (ε_{ijk}). The residual would be analyzed for the inherent spatial structure of the variable at that location. The less formal approach to resistant methods by *Cressie* [1984, 1986] was adopted. It is, however, always a concern that the removal of the mean or the median might introduce bias into

the data. However, *Cressie and Glonek* [1984] have shown that known bias problems in estimation of the semivariograms are greatly ameliorated if medians instead of means are used to define the residuals. Moreover, early studies showed that median polish is better than the mean because it is little affected by outlier(s), common in field data [*Hoaglin et al.*, 1983; *Cressie and Glonek*, 1984; *Mohanty et al.*, 1991]. Therefore the median-polishing techniques were used to polish the data for different additive directional components. Detailed median polish algorithm for a two-way table is defined by *Emerson and Hoaglin* [1983, p. 166] and *Cressie* [1991, p. 186]. As in the work by *Cook* [1985], a median polish algorithm for a three-dimensional grid was established in this study. This polishing could be achieved either (1) with the algorithm that successively removes the row and column medians until there is no further change in residuals for each horizontal layer and then removes the layer median or (2) with the algorithm that successively removes the row, column, and layer medians until no further change in residuals. Whatever route we took, however, the residuals remain the same at end of the median polishing scheme. A schematic flowchart (Figure 2) illustrates the approach adopted for exploratory data analyses and semivariogram estimation. In summary, a ladder of median-polishing algorithms has been developed to iterate the procedure until the mean and the variance along rows, columns, diagonals, and layers attain constancy (i.e., independent of each other) as well as the histogram of residuals looks normal.

Data Check

Exploratory data analyses that rely on graphing are especially suitable for spatial data. Identifying the contaminating outlier(s), directional trends (drift), normality, and dependency of the mean and the variance in the data through suitable plots and graphs yield valuable insights into the problem and aids analysis and interpretation. Frequency plots and median versus interquartile range-squared plots are used to assess data distributions and median and variance (interquartile range squared) constancy or dependency. Plots of median across rows and columns can identify directional trends along both horizontal grid directions. Plots of medians of horizontal layers against depth are used to identify trend in the vertical direction. Diagonal intrinsic trends or cross-product trends of row and column effects along the diagonals of the grid can be examined by plotting the residuals of row and column median polish versus the quadratic term $[(x_i - \bar{x})(y_j - \bar{y})]$.

Spatial Variability

After \log_e transformation and resistant schemes of median polish were used to remove nonstationarity (of the mean and of the variance) and any nonnormality of the data due to extrinsic factors and intrinsic trends, a geostatistical analysis was made to study the spatial variability of residual soil nitrate concentration based on this three-dimensional homogenized residual set. Figure 2b shows the steps involved in computing the composite three-dimensional semivariogram. Initially proposed by *Myers and Journel* [1990] to model zonal anisotropy, the composite three-dimensional semivariogram is primarily a combination of the average one-dimensional horizontal semivariograms ($\bar{\gamma}(h_x)$ in the x direction and $\bar{\gamma}(h_y)$ in the y direction) and the average one-dimensional vertical semivariogram ($\bar{\gamma}(h_z)$ in the z di-

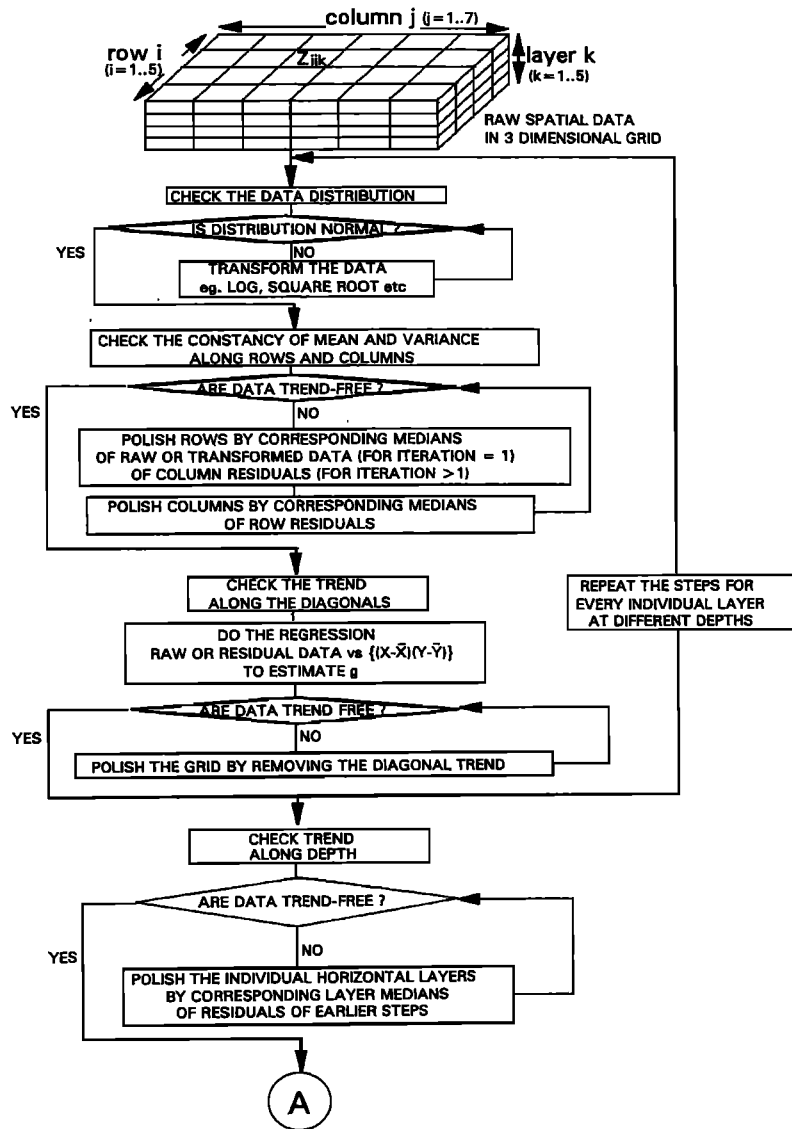


Figure 2a. Schematic flow chart for the three-dimensional resistant median-polishing scheme.

rection) in their respective lag scales, according to the three-dimensional homoscedastic data (residuals). The semivariogram models constructed in this manner will result in conditionally nonnegative definite models and as a consequence to noninvertible kriging matrices. However, nonnegative definite models are sufficient conditions in this application as we did not use semivariogram models for kriging purposes. This three-dimensional spatial variability phenomenon can also be interpreted as geometric anisotropy in three directions (i.e., x, y, and z).

Composite Three-Dimensional Semivariogram

Define

$$\gamma(h_x, h_y, h_z) = \gamma(h_x) + \gamma(h_y) + \gamma(h_z). \quad (2)$$

In addition, two-dimensional horizontal isotropic sample semivariograms ($\gamma^*(h_x, h_y)$) were computed for comparison purposes.

The classical semivariogram estimator as developed by

Matheron [1963] was used to estimate two- and one-dimensional semivariograms:

$$\gamma^*(h_i) = \left\{ \frac{1}{2N(h_i)} \sum_{i=1}^{N(h_i)} [Z(x) - Z(x + h_i)]^2 \right\}, \quad (3)$$

where

- $\gamma^*(h)$ estimate of $\gamma(h)$ for lag distance class h_i ;
- $Z(x)$ measured sample value at point x ;
- $Z(x + h_i)$ measured sample value at point $x + h_i$;
- $N(h_i)$ total number of sample pairs for the lag class h_i .

Average two-dimensional horizontal isotropic sample semivariogram $\bar{\gamma}^*(h_i)$ was calculated as the weighted average of the individual two-dimensional horizontal isotropic sample semivariograms $\gamma_k^*(h_i)$ at different soil horizons, based on the number of pairs $N_k(h_i)$ at each lag class (h_i) [Journal and Huijbregts, 1978, p. 213; Cressie, 1985]. Define

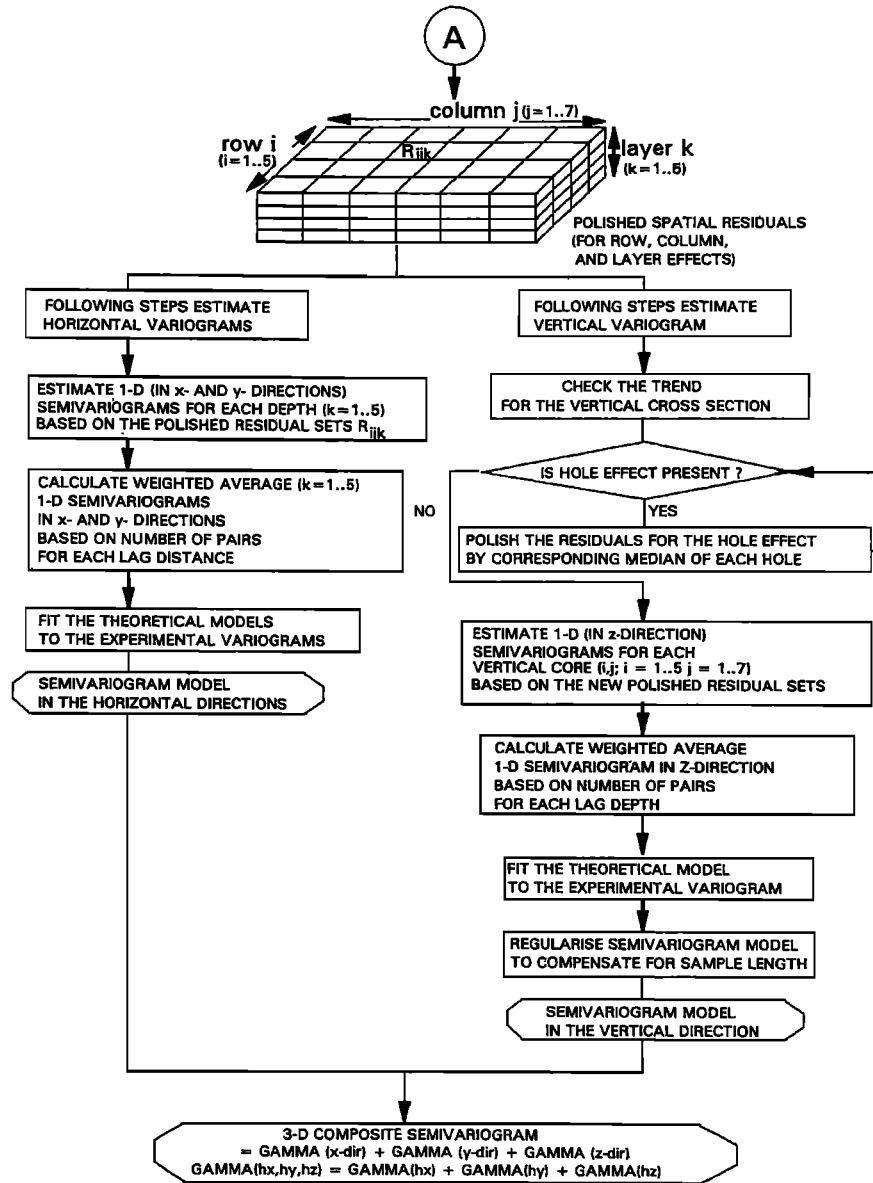


Figure 2b. Schematic flowchart for the semivariogram analyses adopted for the data when arranged on a three-dimensional grid.

		number of pairs	lag class
Layer 1:	$\gamma_{k=1}^*(h_i)$	$N_{k=1}(h_i)$	$i = 1 \dots n;$
Layer 2:	$\gamma_{k=2}^*(h_i)$	$N_{k=2}(h_i)$	$i = 1 \dots n;$
.	.	.	.
.	.	.	.
Layer K:	$\gamma_{k=K}^*(h_i)$	$N_{k=K}(h_i)$	$i = 1 \dots n;$

Average two-dimensional horizontal isotropic sample semivariogram:

$$\bar{\gamma}^*(h_i) = \frac{\sum_{k=1}^K \gamma_k^*(h_i) N_k(h_i)}{\sum_{k=1}^K N_k(h_i)} \quad i = 1 \dots n. \quad (4)$$

Similarly, one-dimensional semivariograms ($\gamma^*(h_x)$, $\gamma^*(h_y)$, and $\gamma^*(h_z)$) can be estimated for each soil layer and vertical cross-sectional face parallel to rows (or columns) using the two-dimensional semivariogram estimators but limiting the estimation to one direction (x, y, or z). Before estimating the one-dimensional vertical semivariogram, however, the preferential or nonpreferential movement of NO₃-N, i.e., sample hole effect, should be polished by medians, if present, by examining the median of each sample hole across the vertical cross-sectional face. Like the average two-dimensional horizontal isotropic sample semivariogram, the average one-dimensional sample semivariograms ($\bar{\gamma}^*(h_x)$, $\bar{\gamma}^*(h_y)$, and $\bar{\gamma}^*(h_z)$) were calculated as a weighted average of one-dimensional sample semivariograms over the number of horizontal layers or vertical faces. This average semivariogram estimation (of the residuals of three-dimensional median polish approach) is, however, based on the assumption that the individual horizontal layers or ver-

Table 1. Statistical Parameters of NO₃-N Concentration Under Conventional Tillage and No-Tillage Systems

Depth, cm	Mean	Median	Standard Deviation	Coefficient of Variation, %	Minimum	Maximum
<i>Conventional Tillage, NO₃-N Concentration, mg/L</i>						
30	19.34	17.30	13.69	70.79	5.50	83.30
60	14.39	13.40	6.75	46.93	7.20	38.80
90	8.16	7.70	2.81	34.45	3.50	14.20
120	10.19	9.30	3.87	37.97	4.90	22.30
150	11.85	11.30	2.43	20.48	6.60	17.70
<i>No-Tillage, NO₃-N Concentration, mg/L</i>						
30	18.40	18.20	5.58	30.32	8.40	33.30
60	11.74	10.70	4.89	41.67	3.70	24.40
90	10.11	10.30	3.30	32.58	1.90	16.50
120	9.21	9.00	3.04	32.98	3.30	16.30
150	9.14	8.80	2.86	31.31	4.00	17.70

tical cross sections are intrinsic random fields. By this composite three-dimensional semivariogram approach not only did we increase the dimensions of prediction but also we achieved more accurate semivariogram estimates for each lag class as they are based on a greater numbers of pairs (by averaging over horizontal layers or vertical faces). Different theoretical models with or without sill and definite range, such as nugget, linear, and spherical models were used to describe spatial structure fitting the one-dimensional average sample semivariograms. Vertical semivariogram models, however, were regularized to compensate for the vertical sample length of 10 cm.

Results and Discussion

Various statistical parameters for NO₃-N levels at various depths and tillage systems were estimated and compared (Table 1). Some important observations were made based on the values of these statistical parameters. Consistent decreases in nitrate levels with depth to 90 cm and reaccumulation and more stable distribution of NO₃-N between 90- and 150-cm depths for conventional tillage system are two noticeable features. Under the no-tillage system, a similar phenomenon was observed, but it was more stable with depth.

As was mentioned earlier, our experimental grid design was made in purposeful directions with grid rows parallel to crop rows in the plot. Hamlett *et al.* [1986] and Cressie and Horton [1987] have reported that crop rows contribute to differences in soil hydrologic properties. Similar effects are also possible on the distribution of NO₃-N in the soil profile because of plant extraction and biological processes. Therefore medians of parallel rows were used to "polish" the data to remove the possible crop row effect. Figure 1 shows the location of existing subsurface tile lines in the tillage plots. Because tile lines are present in the center of plots and parallel to row crops, an elliptical shape water table develops during high rainfall (and so high water table). This causes preferential movement of NO₃-N toward the tile line in the soil profile in a parallel study by the authors (B. P. Mohanty and R. S. Kanwar, Spatial variability of nitrate-nitrogen and moisture content in the soil profile of a tile-drained agricul-

tural field: Coregionalization, submitted to *Water Resources Research*, 1993). This movement may cause an uneven distribution of residual NO₃-N in the soil profile. Therefore polishing the columns perpendicular to the tile line would remove any possible tile-induced effect or any other trend in that direction.

Initially, soil NO₃-N concentration data were examined for additivity of small effects (normality) at each horizontal layer at different depths under both conventional tillage and no tillage. In most instances, these conditions could not be satisfied. Therefore log_e transformations were made to achieve normality if the data were lognormally distributed. Because most soil NO₃-N concentration data were found lognormally distributed, all further analyses of resistant techniques were made using the log_e-transformed data. Besides additivity in small effects (normality), additivity of small effects to large effects (homogenous variances) is usually achieved by log_e transformation of the data [Cressie, 1985; Hamlett *et al.*, 1986]. Cressie [1985] clearly showed the advantage of (combined) weighted average semivariograms based on the transformed grades over scaled (relative) semivariograms across regions. Our study also revealed that log_e transformation can be used as a variance-controlling transformation.

Detrending

Log_e-transformed soil nitrate concentration data were examined for stationarity or possible trend in the median along the two major directions of the grid (i.e., along the row and the column). Medians of five rows and seven columns were plotted across the respective rows and columns to investigate any nonstationarity (or trend) along directions parallel to grid columns and rows, respectively. In both tillage practices (no tillage and conventional tillage) and all five horizontal layers (at 30-, 60-, 90-, 120-, and 150-cm depths), nonstationarity was more the rule than the exception. We picked up one example, arbitrarily, to show the nonstationarity in the median along rows and columns. Figure 3 shows that medians along rows and columns for the horizontal layer at 90-cm depth under conventional tillage are nonstationary and have definite trends in both row and

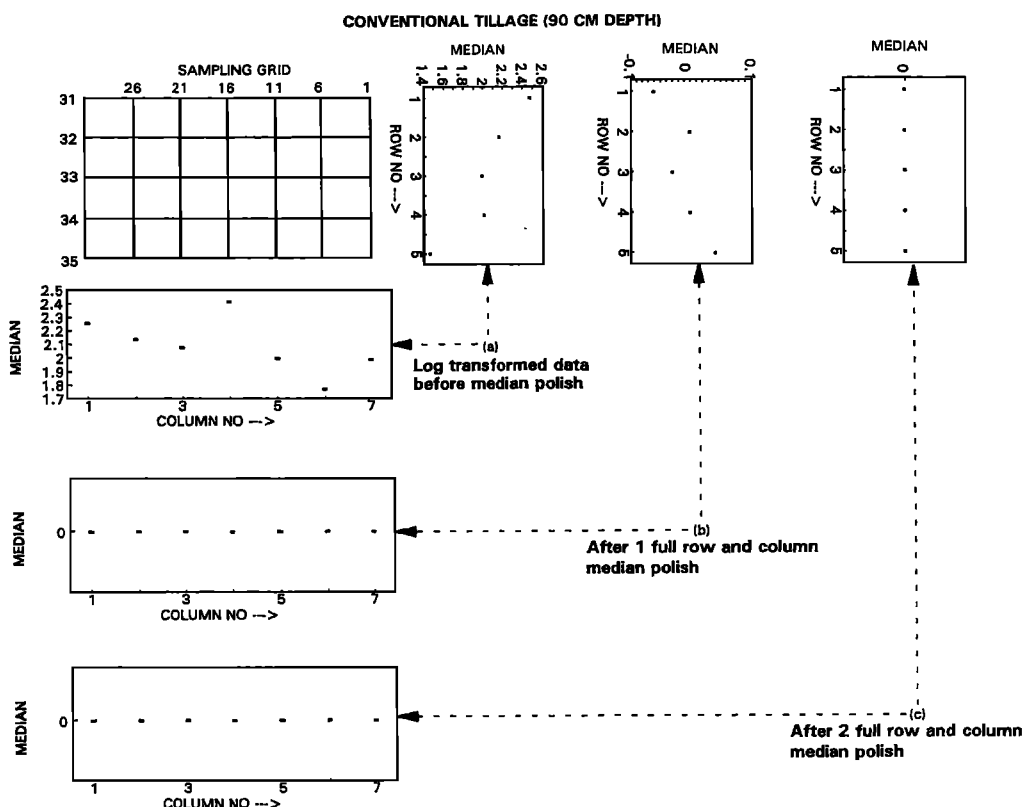


Figure 3. (a) Nonstationarity in the median of \log_e -transformed data, indicating trend in row and column directions; (b) medians along row and column directions after one full step sweep; (c) medians along row and column directions after two full step sweeps, indicating complete stationarity in the median.

column directions with occasional bounce. The directions of increasing or decreasing trend, however, were inconsistent for different horizontal layers, under both tillage practices. Medians of soil nitrate concentration of horizontal layers at different depths were plotted against the depth (e.g., no tillage; Figure 4) to illustrate any trend in the vertical direction. As expected, nonstationarity in the median (trend in the vertical direction) prevailed in the data.

To check the homogeneity of variance, median versus interquartile range squared was plotted; these plots are shown in Figure 5 for no tillage and conventional tillage. Each point results from every row and every column of every horizontal layer for a total of 60 [= (5 + 7) × 5] points. Nonstationarity in variance for the measured $\text{NO}_3\text{-N}$ data is evident from Figure 5. The degree of nonstationarity, however, is more prominent under conventional tillage than no tillage. The plots also show that the relation between median and interquartile range squared is proportional for conventional tillage, whereas the relation is relatively more stable for no tillage. Our objective is to use a resistant approach to remove these mean and variance nonstationarities and trends along the three major axes (row, column, and depth). Once trends along three major axes are removed from data, any diagonal trends present (trends along the diagonal directions of the horizontal grid) need to be investigated and removed. This whole procedure will generate a trend-free (composite) data set for geostatistical analysis.

Figure 5 was used to compare nonstationarity in variances before and after the \log_e transformation. It is evident from

these plots that \log_e transformation has reduced nonstationarity in the variance. Median polish was conducted for rows and columns at each depth for both the no tillage and conventional tillage plots. Medians are plotted across rows and columns (polished for rows followed by columns) as well as for two full sweeps (polished twice, for rows followed by columns) when constancy in median was attained in this particular instance (90 cm depth, conventional tillage). In most layers, no change in medians occurred after two full sweeps. In a few layers, constancy in median was attained after one full or one and one half sweeps. Usually, however, the directional trends are removed in the first sweep, and (any) residual effects are removed in the following sweeps. By comparing Figures 3a, 3b, and 3c, the measured data were gradually cleaned up for the trends along crop row and its perpendicular direction. Moreover, Figure 6 was plotted to provide a three-dimensional view of the measured data and the residuals achieved along the route of resistant analysis; it shows that the \log_e transformation [$\log_e(Z_{ijk})$] tends to squeeze the high values and spread out the small values of raw (measured) data, which makes better stationarity in the variance. Furthermore, median polish by row and column sweeps removes directional trends (nonstationarity in the median) and makes the data [$\log_e(\epsilon_{ijk})$] smoother and more homoscedastic, except for a few spatial outliers. However, *Gotway and Cressie* [1990] pointed out that these spatial outliers need careful examination before removing them from further analyses, which might provide some important information.

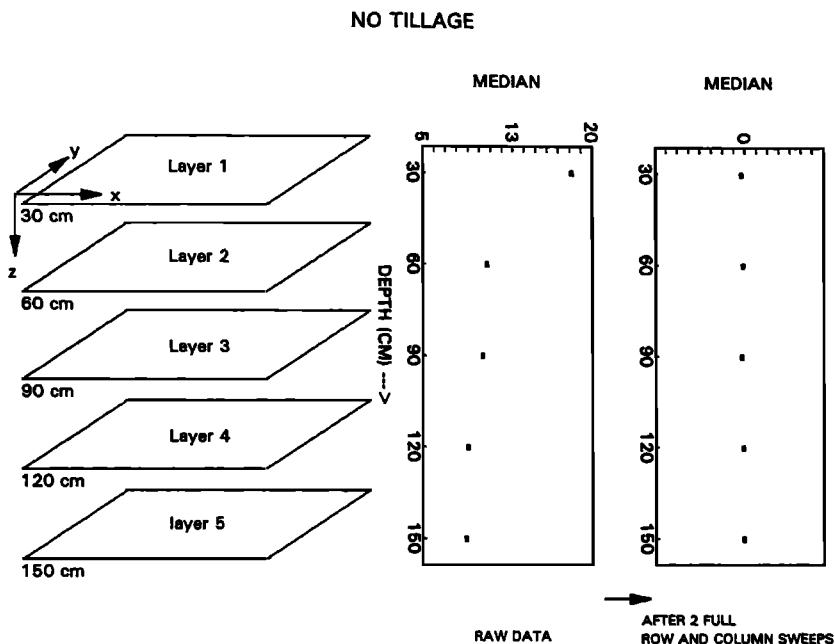


Figure 4. Layer medians in the depth direction before and after \log_e transformation and two full step sweeps. Shows nonstationarity in the median is completely removed by the median polish.

Holes and bumps in residual soil $\text{NO}_3\text{-N}$ data might be showing macropore or channel (causing preferential flow of soluble nitrate) effect and an impervious layer or incomplete mixing of water and nitrate in a given layer due to the effects of macropore flow. Corresponding frequency plots are also presented to show the gradual improvement of normality, and nonstationarity (i.e., the secondary peaks in the histo-

gram) is removed, thereby partly fulfilling our stationarity assumption.

After removing the trends along the rows and columns, the possible presence of diagonal trend was examined by regressing these residuals versus $[(x_i - \bar{x})(y_j - \bar{y})]$. In Figure 7, diagnostic plots show individual depths under both tillage systems. No trend was evident along any diagonal direction

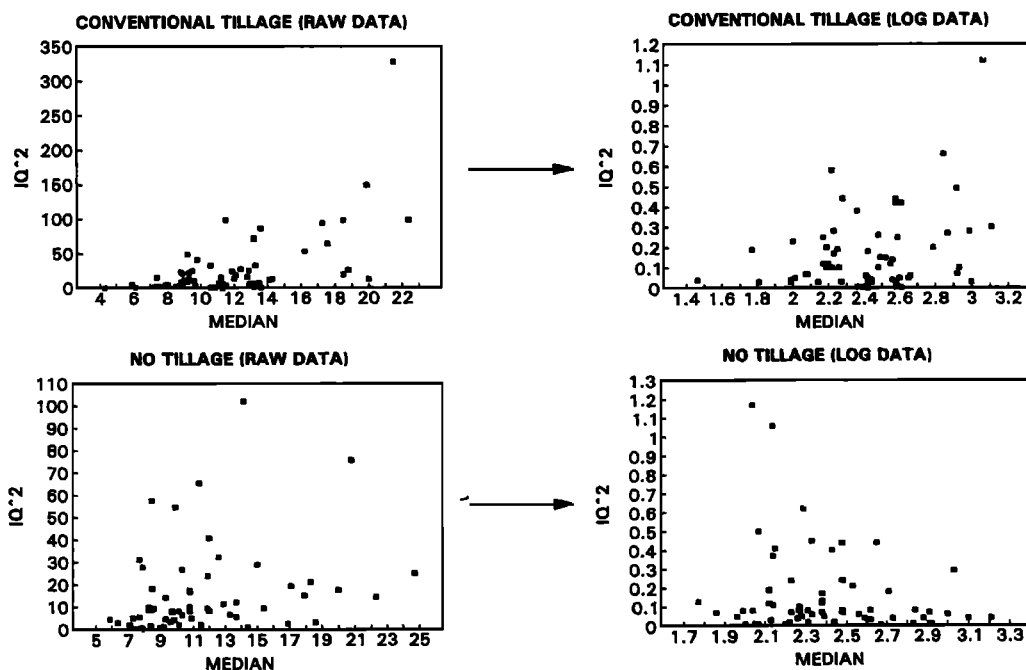


Figure 5. Check for nonstationarity in the variance. Interquartile range squared versus median (spread versus level) demonstrates \log_e transformation as a variance stabilizing transformation.

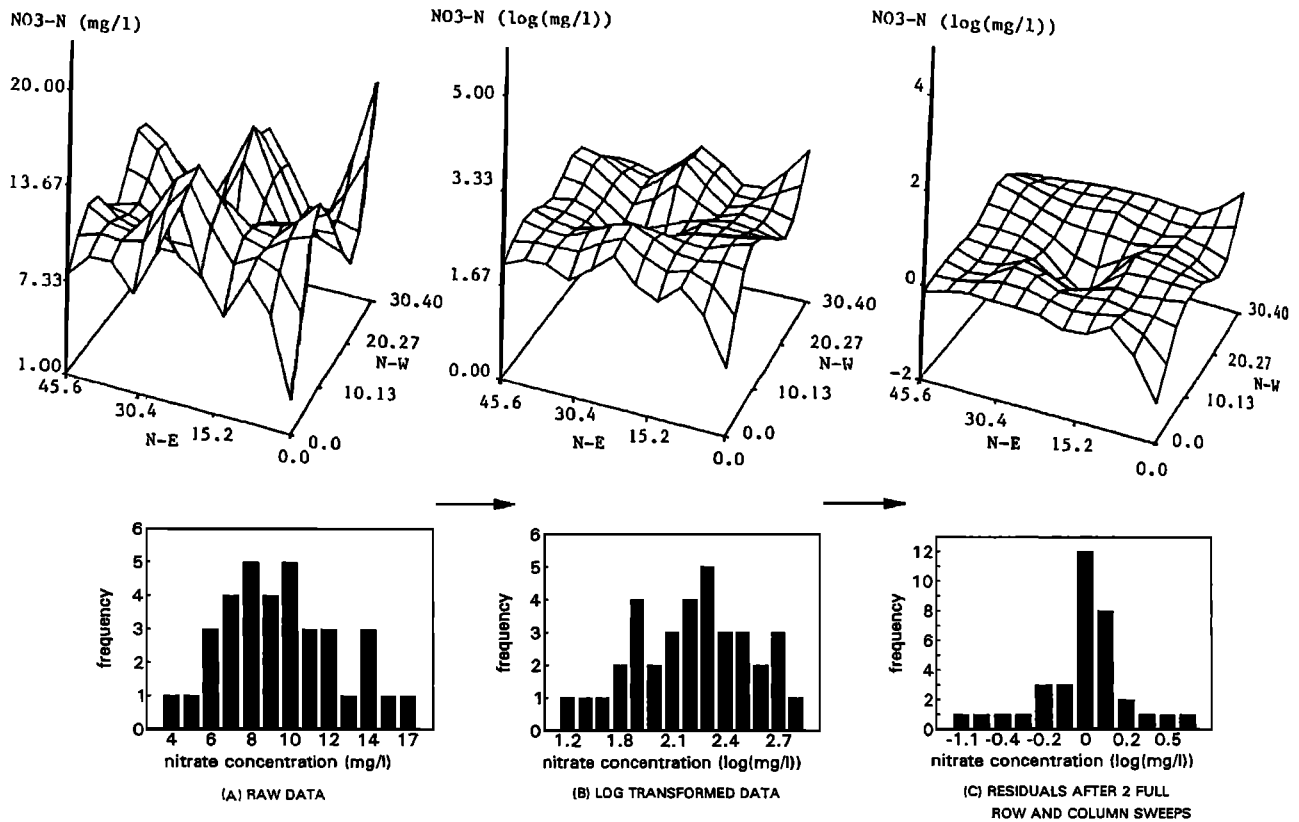


Figure 6. Three-dimensional surface plots and frequency histograms show the gradual improvement of data (normality and stationarity in the mean and the variance) by \log_e transformation and two full step row and column sweeps. This particular case is for no-tillage plot at 120-cm depth. Any hole or bump on the surface (Figure 6c) indicates the location of preferential or nonpreferential $\text{NO}_3\text{-N}$ transport path.

by visual inspection. A maximum fit of $r^2 = 0.15$ with a g (equation (1)) = 0.0068 was evaluated by linear regression for 90-cm depth under the no-tillage system. This reconfirms our visual judgement of no trend along the diagonal (i.e., $g = 0$). After close stationarity was achieved in the mean and the variance in individual layers, in all horizontal directions, the next step was to remove the layer effect (i.e., trend in vertical direction) from the five horizontal data sets, thus making a three-dimensional composite homogenized data set. Individual horizontal layers at different depths were polished by their respective layer medians. Interestingly, we did not find any layer effect remaining in the residuals after one or two rounds of row and column median polish in each individual soil layer. Residuals must become so small and clustery around the median(0) that an evident layer effect no longer exists.

The spatial distribution of residual $\text{NO}_3\text{-N}$ is represented by the additive model (equation (1)), a combination of extrinsic factor(s) contribution(s) along different direction(s), and the spatial structure of the residual term (ε_{ijk}). Separating the common term (μ) and directional components (α , β , and ξ) from the data leaves the residual term (ε_{ijk}) to be analyzed for inherent tillage effect in the spatial variability of residual $\text{NO}_3\text{-N}$. Before the semivariograms for residuals (ε_{ijk}) were estimated, composite residual sets for both tillage practices in three dimensions were reexamined to investigate whether the pooled residuals were near normal with mean zero and variance σ^2 . Residuals had homogenous variance

due to \log_e transformation (Figure 5) and a mean near zero after row, column, and layer medians were removed (Figure 8). These residuals were used to diagnose the spatial structure of residual soil nitrate distribution in horizontal directions under both no tillage and conventional tillage. For the semivariogram in the vertical direction, however, we need one further refinement in the data residuals. Although the residuals have no more directional effects (in x , y , and z directions), they may have some sample hole effects (nonstationarity in the median across sample holes). Hole medians were plotted to investigate the sample hole effect across the vertical faces ($i = 1, \dots, 5$), and nonstationarity was evident in the hole medians shown in Figure 9. This effect was removed by sweeping the holes once by their respective medians. Now these new residuals were used to infer the spatial structure of soil nitrate distribution in the vertical direction (z direction) under both tillage practices.

Semivariogram Analysis

Two-dimensional horizontal isotropic sample semivariogram. After examining and removing nonnormality and nonstationarity in the mean and the variance of data sets, semivariograms were estimated by the classical semivariogram estimator (equation (3)). Two-dimensional horizontal isotropic (assuming isotropy) as well as directional sample semivariograms (in x and y direction) were computed for individual horizontal layers. Average two-dimensional horizontal isotropic and average directional sample semivariograms (in x and y

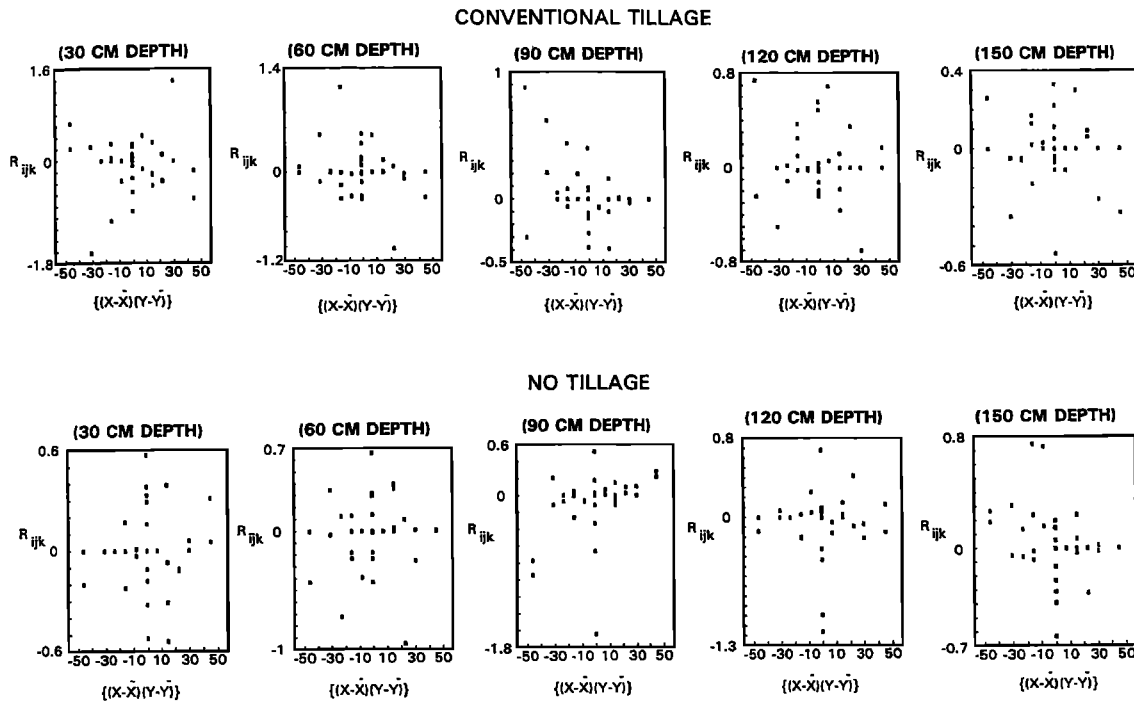


Figure 7. Diagnostic plots to examine the presence of any diagonal trends in the horizontal layers.

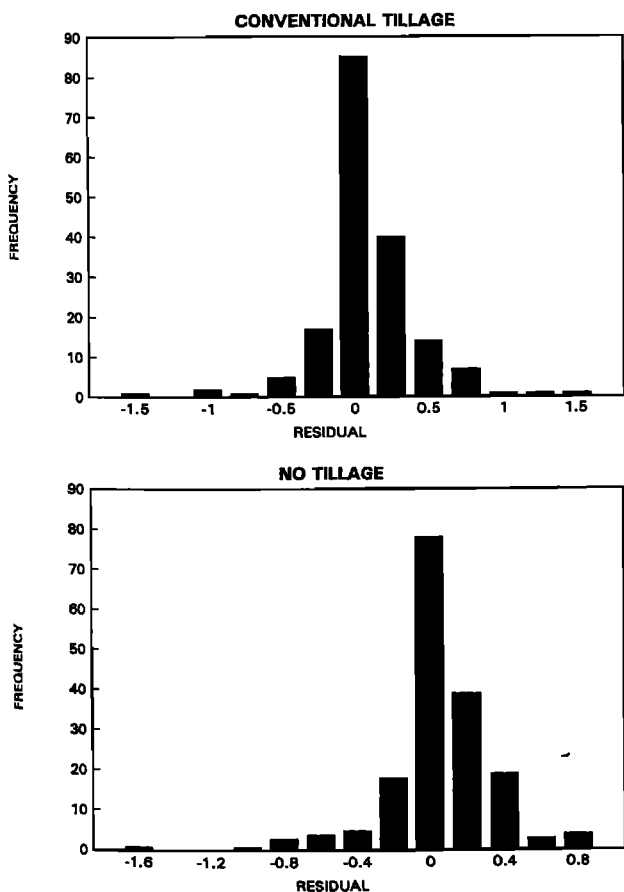


Figure 8. Frequency histogram of the 175 pooled residuals over the three-dimensional grid after executing three-dimensional median-polishing scheme.

direction) were calculated as the weighted average (equation (4)) of these five sets of sample semivariograms. Two-dimensional horizontal isotropic sample semivariograms at different depths and "average two-dimensional horizontal isotropic" sample semivariograms are presented in Figure 10 for both no tillage and conventional tillage plots. A maximum of 760 to a minimum of 360 pairs were used to calculate the

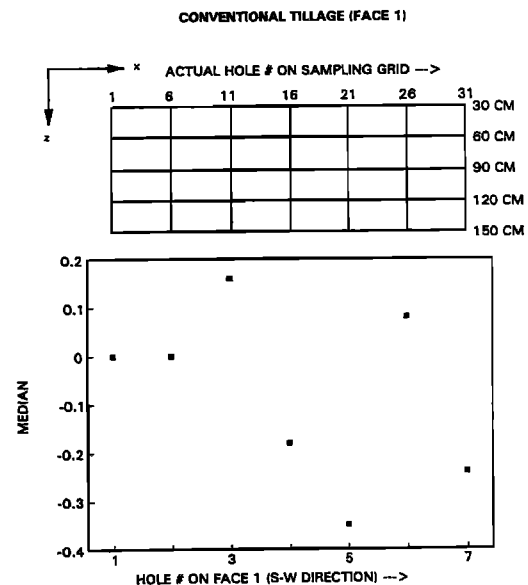


Figure 9. An example of sample hole effect on the vertical face after two full steps of row and column median polish.

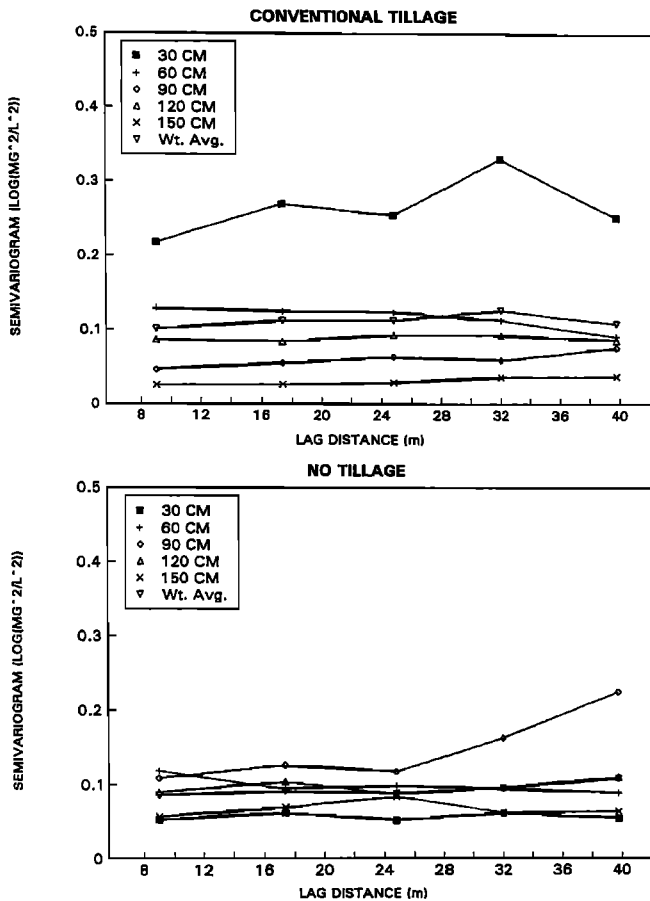


Figure 10. Two-dimensional horizontal isotropic sample semivariograms at different depths and the average two-dimensional horizontal isotropic sample semivariograms under conventional tillage and no-tillage systems. Semivariograms are estimated based on three-dimensional median-polished residuals of the \log_2 -transformed $\text{NO}_3\text{-N}$ (milligrams per liter) data.

average horizontal isotropic sample semivariograms at each lag distance. The number of pairs is about 5 times greater than the number of pairs used for individual horizontal isotropic semivariograms, making the average horizontal isotropic semivariograms more accurate.

Examination of these individual and average isotropic horizontal semivariograms revealed some interesting facts. In conventional tillage, the sill of the semivariogram was relatively much higher at the 30-cm depth than at deeper depths, although the range and the trend (shape) are similar for all these semivariograms. Greater structural variation at the 30-cm depth indicates the tillage-induced variability, which reduced gradually (with the depth with some differences at 90 and 120 cm depths). We suspect that a trace of the effect of tile line (at 120-cm depth) still persists because of the "elliptical" shape of water table (governs the preferential path of $\text{NO}_3\text{-N}$ transport during high water table condition), which could not be removed by three-way main effects only median polish approach. For no tillage, semivariograms are more uniform for all depths except at 90 cm. We suggest the same reasoning of tile-induced "elliptical" water table variability as in case of conventional tillage.

Furthermore, comparing the average two-dimensional horizontal isotropic semivariograms under no tillage with those under conventional tillage (Figure 10), we can infer that soil nitrate distribution under conventional tillage has a small transitive spatial structure and that the distribution under no tillage tends to be more randomly distributed. Under conventional tillage, however, nugget variance is a significant component of the sample semivariogram.

Composite three-dimensional semivariogram. Directional horizontal semivariograms (in x and y directions) were estimated, and "average directional horizontal semivariograms" were calculated as their weighted average (Figure 11). We limited our semivariogram calculation to smaller lags (approximately two thirds of the total lag distance in a particular direction) because they are more accurate and critical for geostatistical interpretation. Visual examination of Figure 11, however, shows evidence of some anisotropy in the semivariograms for conventional tillage practice. Linear structure in the y direction and nugget behavior in x direction were evident from these sample semivariograms. In contrast, the semivariograms showed nugget behavior within very close limits for the no-tillage practice. Similarly, one-dimensional vertical semivariograms (in z direction) were estimated for each vertical cross section. An average one-dimensional vertical semivariogram was calculated as the weighted average over five vertical faces (Figure 11). Figure 11 shows that the spatial structure of soil nitrate distribution is linear on the vertical lag scale for conventional tillage and nugget for no tillage. This structural pattern might result because plowing with conventional tillage distributes soil $\text{NO}_3\text{-N}$ in a more structural fashion than no tillage. Because of plowing, macropores and cracks are destroyed at surface soil layers and become discontinuous at the deeper layers, whose presence or absence is reason for preferential or nonpreferential transport of water and chemicals causing random distribution in space. On the other hand, under no tillage, these factors contribute to nugget behavior in the semivariograms. Similar phenomena were observed in the tillage-induced infiltration studies by *Cressie and Horton* [1987]. Moreover, under conventional tillage, better spatial structure with relatively low nugget effect was found in the vertical direction than in the horizontal directions.

Two composite three-dimensional semivariograms ($\gamma^*(h_x, h_y, h_z)$) are plotted in Figure 12 for both tillage methods by superimposing three one-dimensional average semivariograms ($\bar{\gamma}^*(h_x)$, $\bar{\gamma}^*(h_y)$, and $\bar{\gamma}^*(h_z)$) on the same plot. Horizontal scale indicates both lag depth and lag distance. Lag depth and distances, however, must not be mixed when horizontal or vertical semivariograms are used. Standard theoretical models were used to fit the horizontal and vertical semivariograms to describe their structural patterns. Linear models were adequate for horizontal and vertical semivariograms in conventional tillage, whereas nugget-type models had good fit for no tillage. Interestingly, semivariograms for no tillage in all (three) directions (x , y , and z) were close to one another. The fitted horizontal and vertical semivariogram models for conventional and no tillage are given below:

Conventional tillage, semivariogram model in x direction:

Nugget model

$$\gamma(h_x) = 0, \quad h_x = 0, \quad (5a)$$

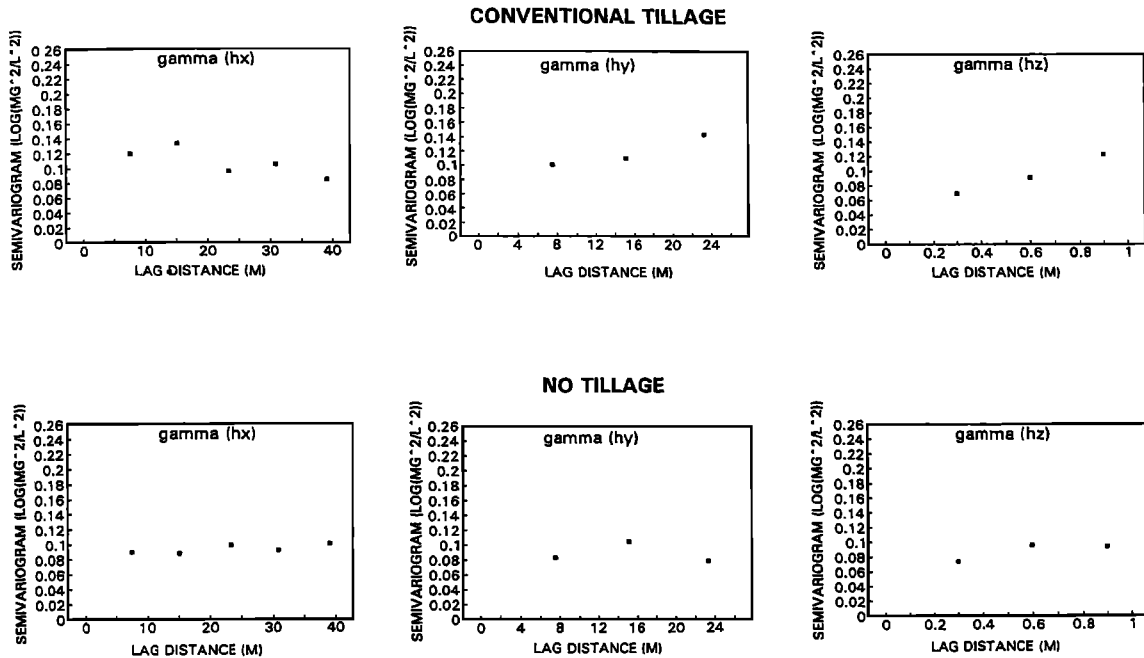


Figure 11. Average directional (x, y, and z) sample semivariograms under conventional tillage and no-tillage systems.

$$\gamma(h_x) = 0.11, \quad h_x > 0. \quad (5b)$$

Conventional tillage, semivariogram model in y direction:

Linear model ($r^2 = 0.92$)

$$\gamma(h_y) = 0, \quad h_y = 0, \quad (6a)$$

$$\gamma(h_y) = 0.076 + 0.0027 h_y, \quad h_y > 0. \quad (6b)$$

Conventional tillage, semivariogram model in z direction:

Linear model ($r^2 = 0.99$)

$$\gamma(h_z) = 0, \quad h_z = 0, \quad (7a)$$

$$\gamma(h_z) = 0.041 + 0.088 h_z, \quad h_z > 0. \quad (7b)$$

Regularizing $\gamma(h_z)$ to compensate for the vertical sample length (0.1 m), the regularized semivariogram ($\gamma_1(h_z)$)

$$\gamma_1(h_z) = 0, \quad h_z = 0, \quad (8a)$$

$$\gamma_1(h_z) = (0.41 + 0.088 h_z)^2(0.259 - 0.088 h_z)/0.03, \quad (8b)$$

$$h_z < 0.1 \text{ m},$$

$$\gamma_1(h_z) = (0.008 + 0.088 h_z), \quad h_z > 0.1 \text{ m}. \quad (8c)$$

No-tillage, semivariogram model in x direction:

Nugget model

$$\gamma(h_x) = 0, \quad h_x = 0, \quad (9a)$$

$$\gamma(h_x) = 0.09, \quad h_x > 0. \quad (9b)$$

No-tillage, semivariogram model in y direction:

Nugget model

$$\gamma(h_y) = 0, \quad h_y = 0, \quad (10a)$$

$$\gamma(h_y) = 0.091, \quad h_y > 0. \quad (10b)$$

No-tillage, semivariogram model in z direction:

Nugget model

$$\gamma(h_z) = 0, \quad h_z = 0, \quad (11a)$$

$$\gamma(h_z) = 0.089, \quad h_z > 0. \quad (11b)$$

Regularizing $\gamma(h_z)$ to compensate for the vertical sample length (0.1 m), the regularized semivariogram ($\gamma_1(h_z)$)

$$\gamma_1(h_z) = 0, \quad h_z = 0, \quad (12a)$$

$$\gamma_1(h_z) = 0.055, \quad h_z > 0. \quad (12b)$$

Composite three-dimensional semivariogram models ($\gamma(h_x, h_y, h_z) = \gamma(h_x) + \gamma(h_y) + \gamma(h_z)$) in conjunction with the additive model (equation (1)) could be used to represent the variability of residual nitrate content in the soil profile. Besides the net advantage of three over two dimensionality, this approach helps to unmask the directional trends of external influences.

Conclusions

Experimental data on $\text{NO}_3\text{-N}$ distribution, arranged on a three-dimensional grid, were used to study the spatial structure of residual $\text{NO}_3\text{-N}$ distribution in the soil profile under conventional tillage and no-tillage plots drained by subsurface tiles. A three-dimensional additive model with quadratic drift (equation (1)) was used to describe the spatial data. Log_e transformation with a three-dimensional median pol-

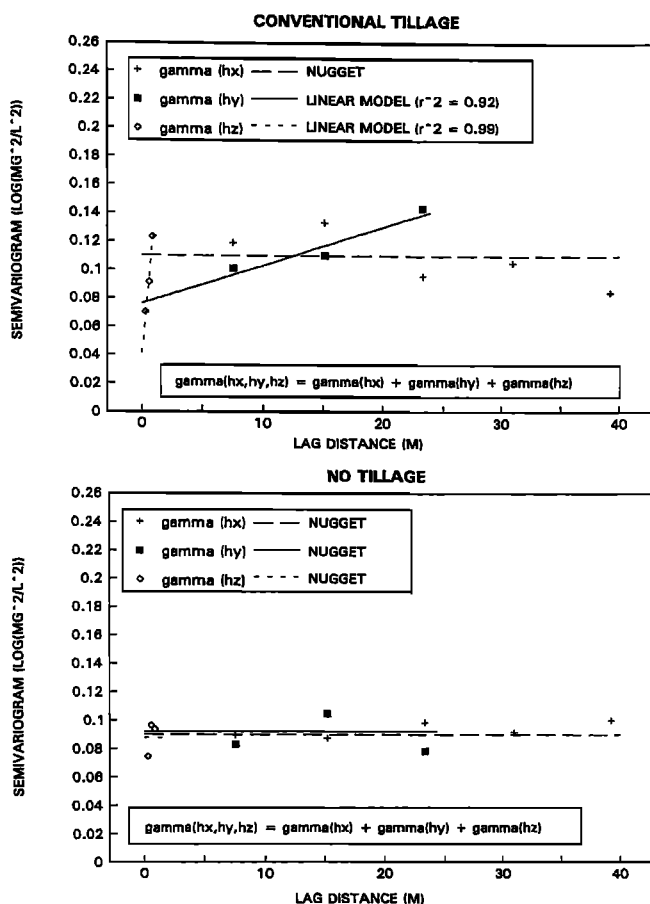


Figure 12. Three-dimensional composite semivariograms (composed of x -, y -, z - directional semivariograms) and fitted models under conventional tillage and no-tillage systems.

ish-resistant scheme was adopted to clean up the data; free the data from directional trends, nonstationarity in the mean, and nonstationarity in the variance; and make the data set more homoscedastic and suitable for geostatistical analyses. The trend-free residuals were used to compute the experimental semivariograms for horizontal layers and vertical faces, and average semivariograms in horizontal and vertical directions were calculated as weighted averages of the individual semivariograms. Two composite three-dimensional semivariograms for conventional tillage and no-tillage were generated by using three one-dimensional semivariograms in the x , y , and z directions with theoretical spatial fitted models. The three conclusions of this study were as follows.

1. At the experimental site, residual $\text{NO}_3\text{-N}$ concentrations in soil decreased to a depth of 90 cm. Beyond this depth, $\text{NO}_3\text{-N}$ concentrations increased. The distribution was gradually uniform for the conventional tillage system and stable for the no-tillage system across the soil profile.
2. Spatial distribution of residual soil nitrate under conventional tillage tends to have linear structures in the horizontal and vertical directions.
3. Compared with conventional tillage, the spatial distribution of residual soil nitrate under no tillage is more random in horizontal as well as vertical directions.

Acknowledgments. We sincerely acknowledge the valuable suggestions of Noel Cressie, Department of Statistics, Iowa State University, for data handling and analyses. Also we express our appreciation to all our anonymous reviewers whose excellent suggestions helped to improve the quality of this paper. This study was partly funded by the Iowa Department of Natural Resources through grant contract 90-6257H-02. Journal paper J-15039 of the Iowa Agriculture and Home Economics Experiment Station, Ames, Iowa.

References

- Baker, D., R. S. Kanwar, and J. L. Baker, Sample volume effect on the determination of nitrate-nitrogen in the soil profile, *Trans. ASAE*, 32(3), 934-938, 1989.
- Baker, J. L., K. D. Campbell, H. P. Johnson, and J. J. Hanway, Nitrate, phosphorus, and sulfate in subsurface drainage water, *J. Environ. Qual.*, 4, 406-412, 1975.
- Beven, K., and P. Germann, Macropores and water flow in soils, *Water Resour. Res.*, 18, 1311-1325, 1982.
- Burrough, P. A., Problems of superimposed effects in the statistical study of the spatial variation of the soil, *Agric. Water Manage.*, 6, 123-143, 1983.
- Cook, N. R., Three-way analyses, in *Exploring Data Tables, Trends, and Shapes*, edited by D. C. Hoaglin, F. Mosteller, and J. W. Tukey, pp. 125-188, John Wiley, New York, 1985.
- Cressie, N. A. C., Towards resistant geostatistics, in *Geostatistics for Natural Resources Characterization*, edited by G. Verly, M. David, A. G. Journel, and A. Marechal, pp. 21-44, D. Reidel, Norwell, Mass., 1984.
- Cressie, N. A. C., When are relative variograms useful in geostatistics?, *Math. Geol.*, 17, 693-702, 1985.
- Cressie, N. A. C., Kriging nonstationary data, *J. Am. Stat. Assoc.*, 81, 625-634, 1986.
- Cressie, N. A. C., *Statistics for Spatial Data*, 900 pp., John Wiley, New York, 1991.
- Cressie, N. A. C., and F. Glonek, Median-based covariogram estimators reduce bias, *Stat. Probab. Lett.* 2, 299-304, 1984.
- Cressie, N. A. C., and D. M. Hawkins, Robust estimation of the variogram, I, *Math. Geol.*, 12, 115-125, 1980.
- Cressie, N. A. C., and R. Horton, A robust-resistant spatial analysis of soil water infiltration, *Water Resour. Res.*, 23(5), 911-917, 1987.
- Dagan, G., Statistical theory of ground water flow and transport pore to laboratory, laboratory to formation and formation to regional scale, *Water Resour. Res.*, 22, 120s-135s, 1986.
- Emerson, J. D., and D. C. Hoaglin, Analysis of two-way tables by medians, in *Understanding Robust and Exploratory Data Analysis*, edited by D. C. Hoaglin, F. Mosteller, and J. W. Tukey, pp. 166-210, John Wiley, New York, 1983.
- Gast, R. G., W. W. Nelson, and G. W. Randall, Nitrate accumulation in soils and loss in tile drainage following nitrogen application to continuous corn, *J. Environ. Qual.*, 7(2), 258-261, 1978.
- Ginn, T. R., and J. H. Cushman, Inverse methods for subsurface flow: A critical review of stochastic techniques, *Stoch. Hydrol.*, 4, 1-26, 1990.
- Gotway, C. A., and N. A. C. Cressie, A spatial analysis of variance applied to soil-water infiltration, *Water Resour. Res.*, 26(11), 2695-2703, 1990.
- Hamlett, J. M., R. Horton, and N. A. C. Cressie, Resistant and exploratory techniques for use in semivariogram analysis, *Soil Sci. Soc. Am. J.*, 50(4), 868-875, 1986.
- Hoaglin, D. C., F. Mosteller, and J. W. Tukey, *Understanding Robust and Exploratory Data Analysis*, 447 pp., John Wiley, New York, 1983.
- Horowitz, J., and D. Hillel, A critique of some recent attempts to characterize spatial variability, *Soil Sci. Soc. Am. J.*, 47, 614-615, 1983.
- Journel, A. G., and C. J. Huijbregts, *Mining Geostatistics*, 600 pp., Academic, San Diego, Calif., 1978.
- Kanwar, R. S., Tillage and crop rotation effects on groundwater pollution, in *Proceedings of the International Conference on Environmental Pollution*, edited by B. Nath and J. P. Robinson, vol. 2, pp. 802-809, Interscience Enterprises, London, 1991.
- Kanwar, R. S., and J. L. Baker, Long-term effects of tillage and reduced chemical application on the quality of subsurface drainage and shallow groundwater, in *Proceedings of Environmentally*

- Sound Agriculture*, edited by A. B. Del Bottcher, pp. 103–110, Florida Cooperative Extension Service, Institute of Food and Agricultural Sciences, University of Florida, Gainesville, 1991.
- Kanwar, R. S., J. L. Baker, and J. M. Lafen, Nitrate movement through soil profile in relation to tillage system and fertilizer application method, *Trans. ASAE*, 28(6), 1731–1735, 1985.
- Kanwar, R. S., J. L. Baker, and D. G. Baker, Tillage and split N-fertilization effects on subsurface drainage water quality and corn yield, *Trans. ASAE*, 31(2), 453–460, 1988.
- Matheron, G., Principles of geostatistics, *Econ. Geol.*, 58, 1246–1266, 1963.
- Mohanty, B. P., R. S. Kanwar, and R. Horton, A robust-resistant approach to interpret spatial behavior of saturated hydraulic conductivity of a glacial till soil under no-tillage system, *Water Resour. Res.*, 27(11), 2979–2992, 1991.
- Myers, D. E., and A. G. Journel, Variograms with zonal anisotropies and noninvertible kriging systems, *Math. Geol.*, 22, 779–785, 1990.
- Onofiok, O. E., Spatial and temporal variability of some soil physical properties following tillage of a Nigerian Paleustult, *Soil Tillage Res.*, 12, 285–298, 1988.
- Rao, P. S. C., and R. J. Wagenet, Spatial variability of pesticides in field soils: Methods of data analysis and consequences, *Weed Sci.*, 33 (Suppl. 2), 18–24, 1985.
- Rao, P. S. C., P. Nkedi-Kizza, J. M. Davidson, and L. T. Ou, Retention and transformation of pesticides in relation to non-point source pollution from crop lands, in *Agricultural Management and Water Quality*, edited by F. Schaller and G. Bailey, pp. 126–140, Iowa State University Press, Ames, 1983.
- Rao, P. S. C., K. S. V. Edvardson, L. T. Ou, R. E. Jessup, and P. Nkedi-Kizza, Spatial variability of pesticide sorption and degradation parameters, in *Proceedings, Symposium on Evaluation of Pesticides in Groundwater, Symp. Ser.*, American Chemical Society, Washington, D. C., 1985.
- Rouhani, S., and H. Wackernagel, Multivariate geostatistical approach to space-time data analysis, *Water Resour. Res.*, 26(4), 585–591, 1990.
- Rubin, Y., and A. G. Journel, Simulation of non-gaussian space random functions for modeling transport in groundwater, *Water Resour. Res.*, 27(7), 1711–1721, 1991.
- Russo, D., A geostatistical approach to the solute transport in the heterogenous fields and its applications to salinity management, *Water Resour. Res.*, 20, 1260–1270, 1984.
- Russo, D., and M. Bouton, Statistical analysis of spatial variability in unsaturated flow parameters, *Water Resour. Res.*, 28, 1911–1925, 1992.
- Scheffe, H., *The Analysis of Variance*, John Wiley, New York, 1959.
- Shafer, J. M., and M. D. Varljen, Approximation of confidence limits on sample semivariograms from single realization of spatially correlated random fields, *Water Resour. Res.*, 26(8), 1787–1802, 1990.
- Singh, P., R. S. Kanwar, and M. L. Thompson, Measurement and characterization of macropores by using AUTOCAD and automatic image analysis, *J. Environ. Qual.*, 20, 289–294, 1991.
- Tabor, J. A., A. W. Warrick, D. E. Myers, and D. A. Pennington, Spatial variability of nitrate in irrigated cotton, 2, Soil nitrate and correlated variables, *Soil Sci. Soc. Am. J.*, 49, 390–394, 1985.
- Trojan, M. D., and D. R. Linden, Microrelief and rainfall effects on water and solute movement in earthworm burrows, *Soil Sci. Soc. Am. J.*, 56, 727–733, 1992.
- Tukey, J. W., *Exploratory Data Analysis*, Addison-Wesley, Reading, Mass., 1977.
- Unlu, K., D. R. Nielsen, J. W. Biggar, and F. Morkoc, Statistical parameters characterizing the spatial variability of selected soil hydraulic properties, *Soil Sci. Soc. Am. J.*, 54, 1537–1547, 1990.
- Velleman, P. F., and D. C. Hoaglin, *Applications, Basics, and Computing of Exploratory Data Analysis*, 354 pp., Duxbury, Boston, Mass., 1981.
- Villeneuve, J-P., P. Lafrance, O. Banton, P. Frechette, and C. Robert, A sensitivity analysis of adsorption and degradation parameters in the modeling of pesticide transport in soils, *J. Contam. Hydrol.*, 3, 77–96, 1988.
- Wagenet, R. J., and B. K. Rao, Description of nitrogen movement in the presence of spatially variable soil hydraulic properties, *Agric. Water Manage.*, 6, 227–242, 1983.
- Walker, A., and P. A. Brown, Spatial variability in herbicide degradation rates and residues in soil, *Crop Prot.*, 2, 17–25, 1983.

R. S. Kanwar, Department of Agricultural and Biosystems Engineering, Davidson Hall, Iowa State University, Ames, IA 50011.

B. P. Mohanty, U.S. Salinity Laboratory, Agricultural Research Service, U.S. Department of Agriculture, 4500 Glenwood Drive, Riverside, CA 92501.

(Received June 8, 1993; revised September 15, 1993; accepted October 15, 1993.)